Functionalization of Nanofibrillated Cellulose with Silver Nanoclusters: Fluorescence and Antibacterial Activity

Isabel Díez, Paula Eronen, Monika Österberg, Markus B. Linder, Olli Ikkala, Robin H. A. Ras*

Native cellulose nanofibers are functionalized using luminescent metal nanoclusters to form a novel type of functional nanocellulose/nanocluster composite. Previously, various types of cellulose fibers have been functionalized with large, non-luminescent metal nanoparticles. Here, mechanically strong native cellulose nanofibers, also called nanofibrillatedcellulose (NFC), microfibrillatedcellulose (MFC) ornanocellulose, disintegrated from macroscopic cellulose pulp fibers are used as support for small and fluorescent silver nanoclusters. The functionalization occurs in a supramolecular manner, mediated by poly(methacrylic acid) that protects nanoclusters while it allows hydrogen bonding with cellulose, leading to composites with fluorescence and antibacterial activity.

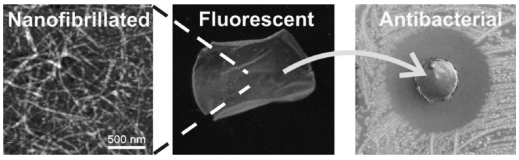

Introduction

Cellulose[1] has attracted interest already long as a widely abundant and sustainable raw material, but more recently also as it is a source of native cellulose nanofibers, also called nanofibrillated cellulose (NFC) (for a comprehensive recent review, see ref.[2]). Different types of native cellulose nanofibers exist, having thicknesses in the nanometer range and different lengths, but they all contain the favorable cellulose I crystalline structure, which allows attractive mechanical properties.[3–5] For example, recently it has been shown that cellulose nanocrystals from tunicates have a very high modulus of ca. 150 GPa.[6] Lower values are reported for cellulose nanofibers.[7,8] The feasible mechanical properties are due to the parallel grossly hydrogen-bonded polysaccharide chains within the native crystalline assemblies. Importantly, the cellulose I crystal structure does not form if dissolution steps are incorporated in the processes. It requires specific processing to produce nanofibers in which the native cellulose I crystalline form is preserved. Long native cellulose nanofibers have been disintegrated from the hierarchical structure of the macroscopic wood fibers by several methods, such as mechanical treatments, chemo-mechanical methods, (2,2,6,6-tetramethylpiperidin-1-yl)oxyl (TEMPO)-mediated oxidation and combination of mild enzymatic hydrolysis combined with high-pressure homogenization, whereas

Dr. I. Díez, Prof. O. Ikkala, Dr. R. H. A. Ras
Molecular Materials, Department of Applied Physics, Aalto University (formerly Helsinki University of Technology), P.O. Box 15100, FIN-02150 Espoo, Finland
E-mail: robin.ras@aalto.fi
I. Díez
Current address: Liquid Crystals and Polymers Group, Departamento de Física de la Materia Condensada, Facultad de Ciencias, Universidad de Zaragoza, C./Pedro Cerbuna 12, 50009, Zaragoza, Spain
P. Eronen, Dr. M. Österberg
Forest Products Surface Chemistry Group, Department of Forest Products Technology, School of Chemical Technology, Aalto University, P.O. Box 16300, FIN-00076 Aalto, Espoo, Finland
Dr. M. B. Linder
VTT Technical Research Center of Finland, Biotechnology, Tietotie 2, FIN-02044, Espoo, Finland

DOI: 10.1002/mabi.201100099

short rod-like cellulose whiskers are obtained by acid hydrolysis.[4,5,9–16] Bacterial cellulose offers another route to native cellulose nanofibers.[1] The native cellulose nanofibers have inspired to pursue towards various functionalities. They allow, e.g., strong nanocomposites, nanopaper, thin films by layer-by-layer assemblies, transparent films, ductile aerogels, low gas-barrier properties and wetting modifications.[17–32] On the other hand, various types of nanoparticles have been assembled on the surfaces of macroscopic and nanoscopic cellulose fibers to allow functionalities, such as antibacterial or catalytic activity and permanent colors.[33–36]

In this work, we aim to explore possibilities to bind metal objects even smaller than nanoparticles, i.e., nanoclusters consisting of only a few atoms, on native cellulose nanofibers. As a characteristic example, silver is an interesting material. Silver nanoparticles show surface plasmon resonance[37] and in catalytic processes it is desirable that the silver particles are small since the surface-to-volume ratio becomes larger, resulting in an enhanced reactivity.[38,39] Also antibacterial properties are obtained when binding silver nanoparticles to cellulose.[40] More generally, now it is established that going down in size to small silver nanoclusters (smaller than 2 nm), composed only of very few atoms, unusual properties are obtained when compared to bulk silver or even silver nanoparticles, for example regarding fluorescence, see recent reviews.[41,42] The bright fluorescence together with the large Stokes shift, the subnanometre size and the low toxicity are the reasons why silver nanoclusters have been studied in regard to biolabelling.[43,44] Fluorescent silver nanoclusters (AgNC) in water solutions are very stable when protected by poly(methacrylic acid) (PMAA)[45] and they display additionally novel properties such as electrochemiluminescence.[46] The optical properties of AgNC are strongly affected by the environment, pointing to the extraordinary sensitivity of the nanoclusters towards the environment.[46–48] Whereas the antibacterial properties of silver nanoparticles have been studied extensively,[49–51] the behavior of fluorescent silver nanoclusters against bacteria has not been described.

Here, we show a facile route to bind silver nanoclusters on native cellulose nanofibers. Besides the characteristic fluorescent properties, the NFC/AgNC composite exhibits a pronounced antibacterial activity, probably due to the large surface area to volume of NFC that favors considerable adsorption of the tiny silver clusters.

Experimental Section

Birch hardwood cellulose disintegrated by mechanical shearing in a high-pressure fluidizer (Microfluidics M-110Y, Microfluidics Corp.Newton, MA) was used. The material passed through the fluidizer 16 times and had a concentration of 1.7 wt% for films used for optical and antibacterial properties. For QCM-D films, cellulose passed through the fluidizer 30 times and had a final concentration of 1.64 wt%. Trimethylsilyl cellulose (TMSC) was synthesized from cellulose powder from spruce (Fluka). Silver nitrate was purchased from Riedel-de Haën (>99.8%), and poly(methacrylic acid) (PMAA, $\overline{M}_w = 100\,000\ g \cdot mol^{-1}$) and polyethyleneimine (PEI, $\overline{M}_w = 50\,000$–$100\,000\ g \cdot mol^{-1}$) from Polysciences. All chemicals were used as received. Water was purified by a Milli-Q system (Millipore).

NFC films (for optical measurements and bacterial test) were cast onto glass substrates and dried at about 40 °C. Silver nanoclusters solutions were synthesized from $AgNO_3$ and PMAA at molar ratios Ag/methacrylic acid (MAA) of 2, 4, 8 as described by Díez et al.[46] Composites of NFC and fluorescent silver nanoclusters were prepared by immersing free-standing NFC films into aqueous silver nanocluster solutions under shaking in darkness. After several hours, the films were thoroughly rinsed with water and dried at ambient conditions.

Fluorescence spectra were obtained with a Varian Cary Eclipse fluorescence spectrometer. Scan speed was $120\ nm \cdot min^{-1}$.

NFC films (for QCM-D) were prepared on silica-coated quartz crystals (QSX303, Q-Sense) by applying the method described previously[52] except that PEI was used as the anchoring layer. Langmuir-Schaefer cellulose films were prepared by deposition of TMSC on polystyrene spin-coated gold crystals (QSX301, Q-Sense) using the horizontal dipping system (KSV Instruments LTD, Helsinki, Finland.[53] 30 layer films were deposited and converted to cellulose prior stabilization by desilylation in 10 wt% HCl-vapor for 5 min. Both films were stabilized in MilliQ-water overnight, and measurements were not started until stable baseline was acquired. A solution of PMAA-protected silver nanoclusters (molar ratio Ag:MAA 2:1) and a solution of PMAA ($2.5\ mg \cdot mL^{-1}$) were pumped through the chambers at constant flow rate of $0.1\ mL \cdot min^{-1}$ and the temperature was kept constant at 24 °C.

The binding of AgNC to NFC was studied with an E4 quartz crystal microbalance with dissipation (QCM-D), manufactured by Q-Sense AB, Västra Frölunda, Sweden. The instrument measures the resonance frequency of oscillation of the quartz crystal with fundamental frequency (5 MHz) and selected overtones (15, 25, 35, 45, 55 and 75 MHz). The adsorbed mass was estimated from the frequency change using the Sauerbrey equation.[54] This equation is strictly valid only for rigid layers and in addition also the bound water is included in the apparent mass detected using QCM-D. However, for comparison, the equation is very useful.

The dried NFC films prepared on QCM-D crystals were characterized with atomic force microscopy (AFM) using a Nanoscope IIIa Multimode scanning probe microscope (Digital Instruments, Santa Barbara, CA). Imaging was performed in room temperature using tapping mode and standard silicon cantilevers (NSC15/AIBS, MikroMasch, Tallinn, Estonia) with resonance frequency around 325 kHz. After measuring, images were flattened to correct for the nonlinearity of the scanner movement.

The effect of NFC/AgNC films on bacteria was tested by growing *Escherichia coli* (XL-1 Blue) in LB-medium and plating on LB-agarose Petri dishes.[55] A series of plates with ten-fold dilutions were prepared (10^{-1}, 10^{-2}, 10^{-3}, 10^{-4}, 10^{-5}). Dried NFC/AgNC films were placed on the agarose gel and incubated at 37 °C for 24 h. Images of the plates were recorded and analyzed. For comparison, a pure NFC

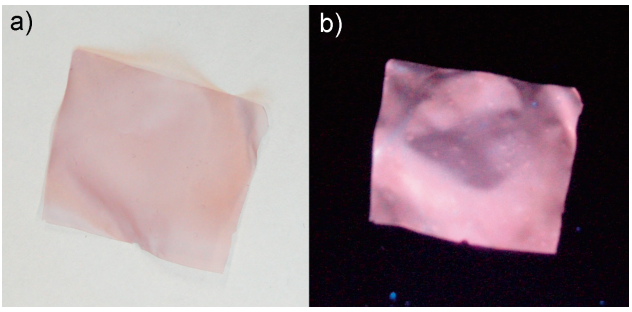

Figure 1. Photographs of an NFC film functionalized with fluorescent silver nanoclusters under (a) white light and (b) UV-light.

was also tested, after being immersed in pure water solution for 60 h, similarly as the NFC/AgNC films, to ensure comparable rinse of the bactericide contained in the nanocellulose solution.

Results and Discussion

The preparation of aqueous solutions of AgNC protected by PMAA was reported elsewhere.[46] Briefly, a solution of silver salt is mixed with a solution of PMAA and the mixture is subsequently irradiated with white light, until pink fluorescent silver nanoclusters are formed. For the preparation of NFC/AgNC composite, NFC films were casted onto glass substrates and dried at about 40 °C. The free-standing films were dipped into a fluorescent silver nanocluster solution for several hours. After carefully rinsing with water, we observed that the films had a homogeneous pink colouration and were luminescent, as shown in Figure 1, thus suggesting that the AgNC/PMAA adducts were successfully connected to NFC.

Optical Properties

Optical characterization demonstrates that the emission intensity and emission wavelength of the NFC/AgNC composite are strongly affected by various synthetic parameters. Here, we will discuss two factors, the first one is the molar ratio Ag:MAA of the AgNC solution used to dip the NFC films. As shown in Figure 2a, the emissive properties of the composite are quite strong when the films were immersed in AgNC solutions with molar ratios Ag:MAA 4:1 and 8:1, but quite weak when immersed in solutions with molar ratio 2:1. These data correspond well with the intensity of the starting solutions, which increases with the molar ratio Ag:MAA. The emission wavelength of the solid composites is located at about 622 nm for all the molar ratios, whereas for the AgNC solutions a red shift with increasing Ag:MAA was reported.[46] In both cases the excitation wavelength is constant for all the molar ratios described here, i.e., in solution the Stokes shift increases

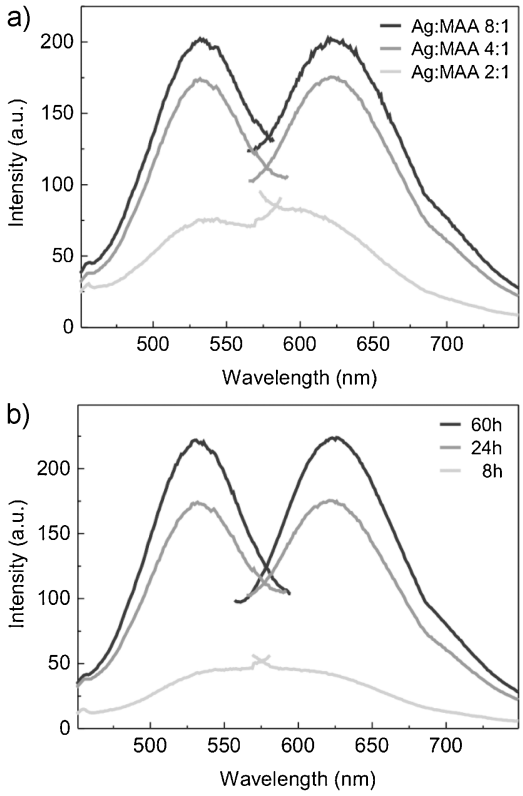

Figure 2. Excitation (recorded at the emission of 620 nm) and emission (recorded at the excitation of 530 nm) spectra of NFC films functionalized with fluorescent silver nanoclusters. (a) Films dipped for 24 h in AgNC solutions with molar ratios Ag:MAA 8:1, 4:1 and 2:1. (b) Films dipped in AgNC solutions with molar ratio Ag:MAA 4:1 for 8, 24 and 60 h.

with concentration, whereas in films it remains constant and smaller, which could be attributed to a smaller interaction nanoclusters/medium in the solid matrix compared to that in the liquid.

A second factor affecting the optical properties is the dipping time. As shown in Figure 2b for films dipped in a AgNC solution with molar ratio Ag:MAA 4:1 the emission intensity of the films increases with the immersion time.

Mechanism of Composite Formation Between Native Cellulose Nanofibers and Silver Nanoclusters

There are a few possible mechanisms for how AgNC are bound to the cellulose surface. The binding of AgNC to NFC could initially be explained in terms of silver affinity. AgNC solutions were prepared using $AgNO_3$ as precursor and PMAA as the initial scaffold. AgNC in solution cannot exist as such; a protecting scaffold is required for their formation and stabilization, preventing that fluorescent silver nanoclusters aggregate to form larger nanoparticles. Nevertheless, it has been demonstrated that fluorescent

AgNC in solution can transfer from one scaffold to another. For example, AgNC can migrate under the proper conditions from poly(acrylic acid) to oligonucleotides[56] or as described in our previous publications from crowded PMAA chains to empty chains[46] or to oligopeptides,[57] keeping their fluorescence. Additionally it is well known that silver is strongly attracted by cellulose and this has been widely used to synthesize large and plasmonic silver nanoparticles.[50,58–60] In this regard, the formation of the composite NFC/AgNC could hypothetically be due to a transfer of AgNC from PMAA chains to cellulose nanofibers. However, this hypothesis is unlikely because the transfer of AgNC reported in literature is typically accompanied with a large shift in the optical bands, whereas in the present case, the shift observed in the emission peak of AgNC when mixed with NFC dispersions is small (not shown). Since PMAA contains –COOH groups and NFC contains –OH groups as well as –COOH groups due to hemicelluloses, the possibility of hydrogen bonding between PMAA and NFC has to be considered. If the NFC film attracts PMAA chains, which are at the same time bound to AgNC, the resultant NFC film will contain both PMAA and fluorescent AgNC. In order to provide evidence for this mechanism of binding, QCM measurements were carried out.

Figure 3a shows the evolution of the adsorbed mass versus time for AgNC adsorption on an NFC film. The NFC film was equilibrated in water overnight and at $t = 10$ min an aqueous solution containing AgNC (protected by PMAA) was pumped into the chamber for about 20 min. After that, the film was rinsed with pure water ($t = 32$ min). When the AgNC protected by polymer are introduced into the chamber, the film starts to adsorb the solutes quickly and after few minutes the binding kinetics slow down considerably. The strong mass increase is partly due to the adsorption of AgNC as demonstrated before in Figure 1 and 2. The role of PMAA in the adsorbed mass becomes clear in a control experiment, where only a PMAA solution was directed onto an NFC film (black curve). Also in this case the QCM detected adsorption, which means that not only AgNC adsorb onto the NFC film but also PMAA. The mass bound to the NFC film is larger when AgNC are present in the solution. A comparison of the mass adsorbed by an NFC film at $t = 20$ min when using a solution of the pure PMAA ($224\,ng \cdot cm^{-2}$) and a solution of AgNC/PMAA ($550\,ng \cdot cm^{-2}$) indicates that the stoichiometry of the adsorbed fluorescent material does not correspond to the stoichiometry of the AgNC solution. Since the NFC film adsorbs $224\,ng \cdot cm^{-2}$ of pure PMAA, the adsorption of AgNC would be expected to be $784\,ng \cdot cm^{-2}$, because the AgNC solution was prepared with a mass ratio Ag:MAA 2.5:1 (molar ratio Ag:MAA 2:1). Instead, a lower value was measured ($550\,ng \cdot cm^{-2}$). However, the adsorbed mass values are only indicative since the QCM also detects bound water and the amount of bound water in the NFC film may change due to adsorption of AgNC and also the different ionic strengths in PMAA and AgNC-containing solution might affect the swollen state of the NFC film and adsorption.[52]

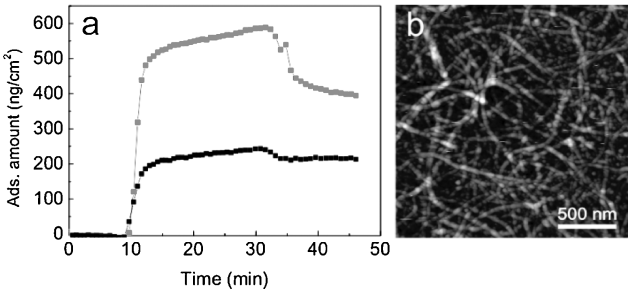

Figure 3. (a) Plot of the adsorbed mass versus time measured by QCM for adsorption of PMAA (black) and PMAA-protected AgNC (molar ratio Ag:MAA 2:1) (grey) from solutions on an ultrathin NFC film. Solutions were pumped in the chamber at $t = 10$ min and rinsed at $t = 32$ min. (b) AFM image of the final NFC/AgNC film.

This suggests that hydrogen bonding between PMAA and NFC facilitates the functionalization of NFC with fluorescent silver nanoclusters. Additional experiments were performed with Langmuir-Schaefer cellulose model films prepared from dissolved cellulose derivative,[53,61] i.e., TMSC. It has the advantages of a smooth surface structure together with well-defined chemistry. Similar results were obtained, indicating that the hydrogen bonds might occur preferentially with the –OH groups of cellulose instead of the –COOH groups from hemicelluloses.

Dried NFC films were imaged using AFM before and after adsorption of PMAA-protected fluorescent silver nanoclusters and no significant differences could be noticed. In Figure 3b the AFM image of the composite NFC/AgNC film is presented. The thin NFC fibers are still clearly observable and no hints of PMAA coils or large aggregated silver nanoparticles can be seen. The absence of large silver particles, although cellulose could act as reducing agent,[60] indicates that silver nanoclusters are well protected by the PMAA.

Antibacterial Properties

The antibacterial behavior of the composites NFC/AgNC were tested against *E. coli* bacteria by the halo method. The composite films for antibacterial testing were prepared by dipping NFC films into AgNC solutions with molar ratios Ag:MAA 8:1, 4:1 and 2:1. For comparison, a pure NFC film was also tested. The agar plates were smeared with *E. coli* bacteria in dilutions from 10^{-1} to 10^{-5}. After allowing the bacteria to grow for 24 h at 37 °C, photographs were recorded. Figure 4 shows an example of the antibacterial behavior of the composite NFC/AgNC prepared from molar

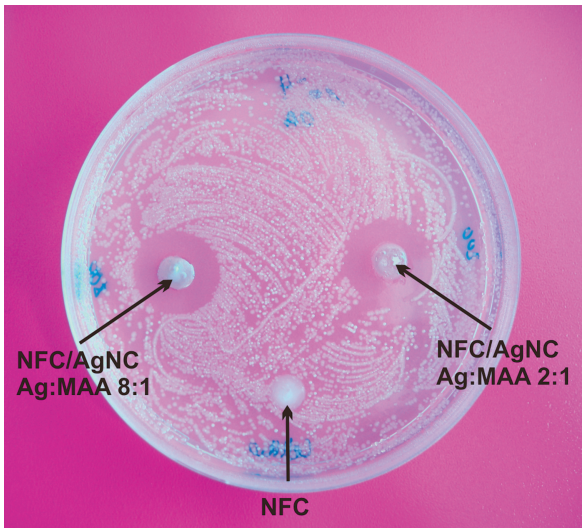

Figure 4. Antibacterial properties of NFC films functionalized with fluorescent silver nanoclusters. *Escherichia coli* bacteria concentration 10^{-4}. Films dipped for 60 h in AgNC solutions with molar ratios Ag:MAA 8:1 (left) and Ag:MAA 2:1 (right); unmodified NFC film (center down).

Table 1. Ratio of the surface area without bacteria over the surface area covered by NFC/AgNC film.

Ratio Ag:MAA[a)]	Bacteria dilution[b)]	Surface area ratio
8:1	10^{-5}	5.0
	10^{-4}	4.9
	10^{-3}	4.3
	10^{-2}	3.5
	10^{-1}	2.8
4:1	10^{-5}	5.3
	10^{-4}	5.4
	10^{-3}	4.9
	10^{-2}	4.1
	10^{-1}	2.7
2:1	10^{-5}	3.9
	10^{-4}	4.8
	10^{-3}	4.4
	10^{-2}	3.7
	10^{-1}	2.8

[a)]Molar ratio of AgNC solution used to prepare the composites; [b)]Serial dilution of bacteria.

ratios Ag:MAA 8:1 and 2:1, compared to the behavior of an NFC film. After incubation, the NFC film shows no antibacterial activity, the bacteria grow freely all around the film. In contrast, around the NFC/AgNC films a large halo free of bacteria can be observed. After incubation, the initially pink NFC/AgNC films were partly metalized, indicating further reduction and aggregation of silver. Nevertheless, silver ions or nanoclusters were released from the film into the gel preventing the growth of bacteria in a large area around the films. The surface without bacterial growth compared to the surface of the NFC/AgNC film for all the samples tested is collected in Table 1. The antibacterial activity is comparable for all the Ag:MAA ratios tested, just slightly larger for the ratio 4:1. The largest area in the agar plate where bacterial growth was completely inhibited is 5.4 times larger than the area of the film causing the effect (Ag:MAA 4:1 and solution of bacteria diluted to 10^{-4}). In this case the thickness of the inhibition halo was 5 mm whereas the radius of the film was only 3.2 mm, which is a much larger effect than reported in literature. For instance, for silver impregnated in glass the values reported are halo 5 mm, film 12.5 mm,[62] for silver impregnated in P_2O_5/SiO_2 they are halo 4.5 mm, film 5.5 mm,[63] for silver solution they are halo 2.5 mm, solution 4 mm,[64] and for AgBr/poly[(4-vinylpyridine)-*co*-(4-vinyl-*N*-hexylpyridinium bromide)]-coated paper they are halo 2 mm, film 5.5 mm.[65] However, we point out that the comparison of the halos with literature values might not be taken entirely quantitative since also other factors can affect dissolution of silver ions, such as time, temperature and pH of the agar.

The release of silver ions or AgNC from the NFC/AgNC film to the gel to prevent bacterial growth takes place only in the presence of water as revealed by the following experiment. When a pink composite NFC/AgNC film is immersed for several days in solvents such as ethanol, methanol, tetrahydrofuran or chloroform, the film keeps the pink color and the fluorescence. In contrast, when immersed in water the film partly looses the pink color while releasing pink AgNC to the solution. The released AgNC in solution are very stable indicating that they are still protected by PMAA, also released from the film.

Conclusion

Native cellulose nanofibers disintegrated from macroscopic cellulose hardwood fibers were successfully functionalized with fluorescent silver nanoclusters by simply dipping a nanocellulose film into a solution of silver nanoclusters protected by PMAA. The mechanism of binding of silver nanoclusters to nanocellulose was discussed and PMAA, carrying silver nanoclusters, was suggested to hydrogen bond to nanocellulose or/and to the residual hemicelluloses, and thus act as mediator in the functionalization. This leads to a novel type of supramolecular native cellulose nanofiber/nanocluster adduct. The composite nanocellu-

lose-nanosilver retains the appealing properties of both components. The high surface area of the nanofibrils favors a significant adsorption of silver nanoclusters that can be released in aqueous medium. The released silver will prevent bacterial growth in a surface area fivefold larger than the area of the film. In conclusion, we have shown that the metal nanocluster/nanocellulose composites are feasible. We expect that such materials are useful in, e.g., wound-healing pads and in more general for other functionalities by selecting different metal nanoclusters.

Acknowledgements: Janne Laine (Aalto Univ.), Timo Koskinen (UPM) and Antti Laukkanen (UPM) are acknowledged for discussions. We acknowledge the Finnish Funding Agency for Technology and Innovation (TEKES) and Academy of Finland for funding. This work has been made within the Finnish Center for Nanocellulosic Technologies (partnership between UPM, Aalto University and VTT).

Received: March 11, 2011; Published online: July 4, 2011; DOI: 10.1002/mabi.201100099

Keywords: bactericides; luminescence; nanocelluloses; nanofibers; nanoclusters

[1] D. Klemm, B. Heublein, H.-P. Fink, A. Bohn, *Angew. Chem., Int. Ed.* **2005**, *44*, 3358.
[2] S. J. Eichhorn, A. Dufresne, M. Aranguren, N. E. Marcovich, J. R. Capadona, S. J. Rowan, C. Weder, W. Thielemans, M. Roman, S. Renneckar, W. Gindl, S. Veigel, J. Keckes, H. Yano, K. Abe, M. Nogi, A. N. Nakagaito, A. Mangalam, J. Simonsen, A. S. Benight, A. Bismarck, L. A. Berglund, T. Peijs, *J. Mater. Sci.* **2010**, *45*, 1.
[3] S. Ahola, M. Österberg, J. Laine, *Cellulose* **2008**, *15*, 303.
[4] H. Yano, J. Sugiyama, A. N. Nakagaito, M. Nogi, T. Matsuura, M. Hikita, K. Handa, *Adv. Mater.* **2005**, *17*, 153.
[5] M. Pääkkö, M. Ankerfors, H. Kosonen, A. Nykänen, S. Ahola, M. Österberg, J. Ruokolainen, J. Laine, P. T. Larsson, O. Ikkala, T. Lindström, *Biomacromolecules* **2007**, *8*, 1934.
[6] S. Iwamoto, W. Kai, A. Isogai, T. Iwata, *Biomacromolecules* **2009**, *10*, 2571.
[7] D. G. Hepworth, D. M. Bruce, *J. Mater. Sci.* **2000**, *35*, 5861.
[8] G. Guhados, W. Wan, J. L. Hutter, *Langmuir* **2005**, *21*, 6642.
[9] A. F. Turbak, F. W. Snyder, K. R. Sandberg, *J. Appl. Polym. Sci.: Appl. Polym. Symp.* **1983**, *37*, 815.
[10] F. W. Herrick, R. L. Casebier, J. K. Hamilton, K. R. Sandberg, *J. Appl. Polym. Sci.: Appl. Polym. Symp.* **1983**, *37*, 797.
[11] K. Fleming, D. G. Gray, S. Matthews, *Chem. Eur. J.* **2001**, *7*, 1831.
[12] A. N. Nakagaito, H. Yano, *Appl. Phys. A: Mater. Sci. Process.* **2004**, *78*, 547.
[13] K. Abe, S. Iwamoto, H. Yano, *Biomacromolecules* **2007**, *8*, 3276.
[14] R. Saito, *Macromolecules* **2001**, *34*, 4299.
[15] M. Henriksson, G. Henriksson, L. A. Berglund, T. Lindström, *Eur. Polym. J.* **2007**, *43*, 3434.
[16] G. Siqueira, J. Bras, A. Dufresne, *Biomacromolecules* **2008**, *10*, 425.
[17] J. R. Capadona, O. van den Berg, L. A. Capadona, M. Schroeter, S. J. Rowan, D. J. Tyler, C. Weder, *Nat. Nanotechnol.* **2007**, *2*, 765.
[18] M. Henriksson, L. A. Berglund, P. Isaksson, T. Lindström, T. Nishino, *Biomacromolecules* **2008**, *9*, 1579.
[19] J. R. Capadona, K. Shanmuganathan, D. J. Tyler, S. J. Rowan, C. Weder, *Science* **2008**, *319*, 1370.
[20] M. Nogi, H. Yano, *Adv. Mater.* **2008**, *20*, 1849.
[21] L. Wågberg, G. Decher, M. Norgren, T. Lindström, M. Ankerfors, K. Axnäs, *Langmuir* **2008**, *24*, 784.
[22] M. Pääkkö, J. Vapaavuori, R. Silvennoinen, H. Kosonen, M. Ankerfors, T. Lindström, L. A. Berglund, O. Ikkala, *Soft Matter* **2008**, *4*, 2492.
[23] H. Fukuzumi, T. Saito, T. Wata, Y. Kumamoto, A. Isogai, *Biomacromolecules* **2009**, *10*, 162.
[24] O. Ikkala, R. H. A. Ras, N. Houbenov, J. Ruokolainen, M. Pääkko, J. Laine, M. Leskela, L. A. Berglund, T. Lindström, G. ten Brinke, H. Iatrou, N. Hadjichristidis, C. F. J. Faul, *Faraday Discuss.* **2009**, *143*, 95.
[25] M. Nogi, S. Iwamoto, A. N. Nakagaito, H. Yano, *Adv. Mater.* **2009**, *20*, 1.
[26] C. Aulin, J. Netrval, L. Wågberg, T. Lindström, *Soft Matter* **2010**, *6*, 3298.
[27] H. Liu, D. Liu, F. Yao, Q. Wu, *Bioresour. Technol. 101*, 5685.
[28] S. Dong, M. Roman, *J. Am. Chem. Soc.* **2007**, *129*, 13810.
[29] A. Walther, J. Timonen, I. Díez, A. Laukkanen, O. Ikkala, *Adv. Mater.* **2011**, DOI: 10.1002/adma.201100580.
[30] M. Kettunen, R. J. Silvennoinen, N. Houbenov, A. Nykänen, J. Ruokolainen, J. Sainio, V. Pore, M. Kemell, M. Ankerfors, T. Lindström, M. Ritala, R. H. A. Ras, O. Ikkala, *Adv. Funct. Mater.* **2011**, *21*, 510.
[31] J. T. Korhonen, P. Hiekkataipale, J. Malm, M. Karppinen, O. Ikkala, R. H. A. Ras, *ACS Nano* **2011**, *5*, 1967.
[32] H. Jin, M. Kettunen, A. Laiho, H. Pynnönen, J. Paltakari, A. Marmur, O. Ikkala, R. H. A. Ras, *Langmuir* **2011**, *27*, 1930.
[33] G. K. Hyde, K. J. Park, S. M. Stewart, J. P. Hinestroza, G. N. Parsons, *Langmuir* **2007**, *23*, 9844.
[34] B. H. Dong, J. P. Hinestroza, *ACS Appl. Mater. Interfaces* **2009**, *1*, 797.
[35] J. P. Hinestroza, *Mater. Today* **2007**, *10*, 64.
[36] C. Chang, J. Peng, L. Zhang, D.-W. Pang, *J. Mater. Chem.* **2009**, *19*, 7771.
[37] K. A. Willets, R. P. Van Duyne, *Ann. Rev. Phys. Chem.* **2007**, *58*, 267.
[38] A. R. Tao, S. Habas, P. Yang, *Small* **2008**, *4*, 310.
[39] N. R. Jana, T. K. Sau, T. Pal, *J. Phys. Chem. B* **1998**, *103*, 115.
[40] H. Dong, D. Wang, G. Sun, J. P. Hinestroza, *Chem. Mater.* **2008**, *20*, 6627.
[41] I. Díez, R. H. A. Ras, "Few-Atom Silver Clusters as Fluorescent Reporters", in *Advanced Fluorescence Reporters in Chemistry and Biology II*, (Ed., A. P. Demchenko), Springer, Heidelberg **2010**, p. 307.
[42] I. Díez, R. H. A. Ras, *Nanoscale* **2011**, *3*, 1963.
[43] J. Zheng, R. M. Dickson, *J. Am. Chem. Soc.* **2002**, *124*, 13982.
[44] J. Yu, S. Choi, C. I. Richards, Y. Antoku, R. M. Dickson, *Photochem. Photobiol.* **2008**, *84*, 1435.
[45] L. Shang, S. Dong, *Chem. Commun.* **2008**, 1088.
[46] I. Díez, M. Pusa, S. Kulmala, H. Jiang, A. Walther, A. S. Goldmann, A. H. E. Müller, O. Ikkala, R. H. A. Ras, *Angew. Chem., Int. Ed.* **2009**, *48*, 2122.

[47] W. Guo, J. Yuan, Q. Dong, E. Wang, *J. Am. Chem. Soc.* **2009**, *132*, 932.
[48] I. Díez, H. Jiang, R. H. A. Ras, *ChemPhysChem* **2010**, *11*, 3100.
[49] I. Sondi, B. Salopek-Sondi, *J. Colloid Interface Sci.* **2004**, *275*, 177.
[50] W. K. Son, J. H. Youk, T. S. Lee, W. H. Park, *Macromol. Rapid Commun.* **2004**, *25*, 1632.
[51] M. Rai, A. Yadav, A. Gade, *Biotechnol. Adv.* **2009**, *27*, 76.
[52] S. Ahola, J. Salmi, L. S. Johansson, J. Laine, M. Österberg, *Biomacromolecules* **2008**, *9*, 1273.
[53] T. Tammelin, T. Saarinen, M. Österberg, J. Laine, *Cellulose* **2006**, *13*, 519.
[54] G. Sauerbrey, *Zeitsch. Phys.* **1959**, *155*, 206.
[55] J. Sambrook, E. F. Fritsch, T. Maniatis, *Molecular Cloning: A Laboratory Manual*, 2nd edition, Cold Spring Harbor Laboratory, Cold Spring Harbor, New York **1989**.
[56] J. Yu, S. Choi, R. M. Dickson, *Angew. Chem., Int. Ed.* **2009**, *48*, 318.
[57] I. Díez, H. Hahn, O. Ikkala, H. G. Börner, R. H. A. Ras, *Soft Matter* **2010**, *6*, 3160.
[58] S. Ifuku, M. Tsuji, M. Morimoto, H. Saimoto, H. Yano, *Biomacromolecules* **2009**, *10*, 2714.
[59] J. H. He, T. Kunitake, T. Watanabe, *Chem. Commun.* **2005**, 795.
[60] J. Cai, S. Kimura, M. Wada, S. Kuga, *Biomacromolecules* **2008**, *10*, 87.
[61] E. Kontturi, M. Österberg, *Model Cellulosic Surfaces*, American Chemical Society, Washington DC **2009**, p. 57.
[62] M. Miola, S. Ferraris, S. Nunzio, P. F. Robotti, G. Bianchi, G. Fucale, G. Maina, M. Cannas, S. Gatti, A. Masse, C. V. Brovarone, E. Verne, *J. Mater. Sci.: Mater. Med.* **2009**, *20*, 741.
[63] H. R. Liu, Q. Chen, L. Song, R. F. Ye, J. Y. Lu, H. P. Li, *J. Non-Cryst. Solids* **2008**, *354*, 1314.
[64] D. C. Tien, K. H. Tseng, C. Y. Liao, T. T. Tsung, *Med. Eng. Phys.* **2008**, *30*, 948.
[65] V. Sambhy, M. M. MacBride, B. R. Peterson, A. Sen, *J. Am. Chem. Soc.* **2006**, *128*, 9798.